npj | Quantum Materials

www.nature.com/npjquantmats

ARTICLE OPEN

Melting of charge order in the low-temperature state of an electronic ferroelectric-like system

Nora M. Hassan[1], Komalavalli Thirunavukkuarasu[2], Zhengguang Lu[3,4], Dmitry Smirnov[3], Elena I. Zhilyaeva[5], Svetlana Torunova[5], Rimma N. Lyubovskaya[5] and Natalia Drichko[1]✉

Strong electronic interactions can drive a system into a state with a symmetry breaking. Lattice frustration or competing interactions tend to prevent symmetry breaking, leading to quantum disordered phases. In spin systems frustration can produce a spin liquid state. Frustration of a charge degree of freedom also can result in various exotic states, however, experimental data on these effects is scarce. In this work we demonstrate how in a Mott insulator on a weakly anisotropic triangular lattice a charge ordered state melts on cooling down to low temperatures. Raman scattering spectroscopy finds that κ-(BEDT-TTF)$_2$Hg(SCN)$_2$Cl enters an insulating "dipole solid" state at $T = 30$ K, but below $T = 15$ K the order melts, while preserving the insulating energy gap. Based on these observations, we suggest a phase diagram relevant to other quantum paraelectric materials.

npj Quantum Materials (2020)5:15 ; https://doi.org/10.1038/s41535-020-0217-5

INTRODUCTION

Frustration of a charge degree of freedom can result in a charge glass[1,2] or a quantum paraelectric state, where electric dipoles fluctuate down to the lowest temperatures[3–5]. Such quantum dipole liquid was observed experimentally in a band insulator on a triangular lattice[4] and in a Mott insulator[6]. Theory predicts that fluctuations of polarization in a band insulator can result in weak ferromagnetism[7], while electric dipole fluctuations coupled to unpaired spins in a Mott insulator can lead to a spin liquid state[5,8]. An experimental realization of a system where electrical dipoles form on a lattice of a Mott insulator at this point is limited to molecular-based systems[3,5,6]. However, exotic multiferroicity[7,9] which can result from an interplay of a quantum paraelectric and a spin liquid is of interest to a broad community working on materials with strong electron-electron interactions. Also, notable is an analogy of a fluctuating charge degree of freedom of a molecular orbital in a quantum dipole liquid to a fluctuating orbital degree of freedom in an orbital liquid in atomic crystals as a way to produce novel spin liquid states[8].

Organic Mott insulators which can host electronic ferroelectricity and quantum dipole liquid are layered charge-transfer crystals based on BEDT-TTF (bis(ethylenedithio)tetrathiafulvalene) molecule. Layers responsible for the interesting physical properties of these materials are formed by (BEDT-TTF)$_2^{+1}$ dimers. They alternate with layers which serve as charge reservoirs and define the exact structural parameters of the BEDT-TTF layers (see Fig. 1a). In the structure of κ-(BEDT-TTF)$_2$Hg(SCN)$_2$Cl (κ-Hg-Cl) discussed in this work, (BEDT-TTF)$_2^{+1}$ sites form a slightly anisotropic triangular lattice. In this compound, electronic ferroelectricity is suggested in a charge ordered state below 30 K[10,11]. In this work we experimentally detect a gradual melting of this charge order as the material is cooled down below 15 K.

Typically, if a system undergoes a phase transition into a broken symmetry state, such as a ferroelectric state, this state is a ground state of the system. A loss of order on lowering temperature, for example, in a re-entrant transition, is very rare to observe experimentally. Such a re-entrant transition was predicted theoretically for some systems with strong electronic interactions[12–15]. In quasi-two-dimensional (quasi-2D) organic metals, a weak re-entrant behavior was observed close to insulating charge order phase for compounds with a quarter-filled conductance band[16].

RESULTS

We use Raman spectroscopy as a main tool for this study. This method provides information about charge state, lattice, and electronic structure of a material through observations of molecular vibrations, phonons, and electronic excitations. In particular, charge distribution in the layer formed by (BEDT-TTF)$_2^{+1}$ molecular dimers is determined by following the frequency of the Raman-active ν_2 stretching vibration of the central C=C bond of the BEDT-TTF molecules (Fig. 1b). This vibration has a known linear dependence on the charge (n) of a BEDT-TTF^n molecule[6,17].

First we will discuss the charge ordered state detected in κ-Hg-Cl below a metal-insulator transition at 30 K[10]. A single ν_2 mode corresponding to (BEDT-TTF)$^{+0.5}$ is observed above the transition temperature (Fig. 1c, $T = 45$ K). In the charge ordered state, where charge symmetry within each dimer site is broken, ν_2 band splits into two vibrational modes detected at 1475 and 1507 cm^{-1}, corresponding to (BEDT-TTF)$^{+0.6}$ and (BEDT-TTF)$^{+0.4}$ on each dimer (Fig. 1c, $T = 20$ K).

Vibrational features in the spectra of κ-Hg-Cl are superimposed on a continuum of electronic excitations, presented in Fig. 2a after subtracting phonon contribution (see Supplemental Information (SI) for the original data). In the (b, c) scattering channel, at the M–I phase transition at 30 K, we observe an opening of an electronic gap. It manifests itself in a suppression of the intensity of the continuum below ~850 cm^{-1} with spectral weight shifted to the region between 850 and 1200 cm^{-1}. While the gap affects electronic states at higher frequencies, the size of the gap 2Δ can be estimated as the frequency where the slope of Raman

[1]Institute for Quantum Matter and Department of Physics and Astronomy, Johns Hopkins University, Baltimore, MD 21218, USA. [2]Department of Physics, Florida AM University, Tallahassee, FL 32307, USA. [3]National High Magnetic Field Laboratory, Tallahassee, FL 32310, USA. [4]Florida State University, Tallahassee, FL 32306, USA. [5]Institute of Problems of Chemical Physics, Chernogolovka, Russia. ✉email: drichko@jhu.edu

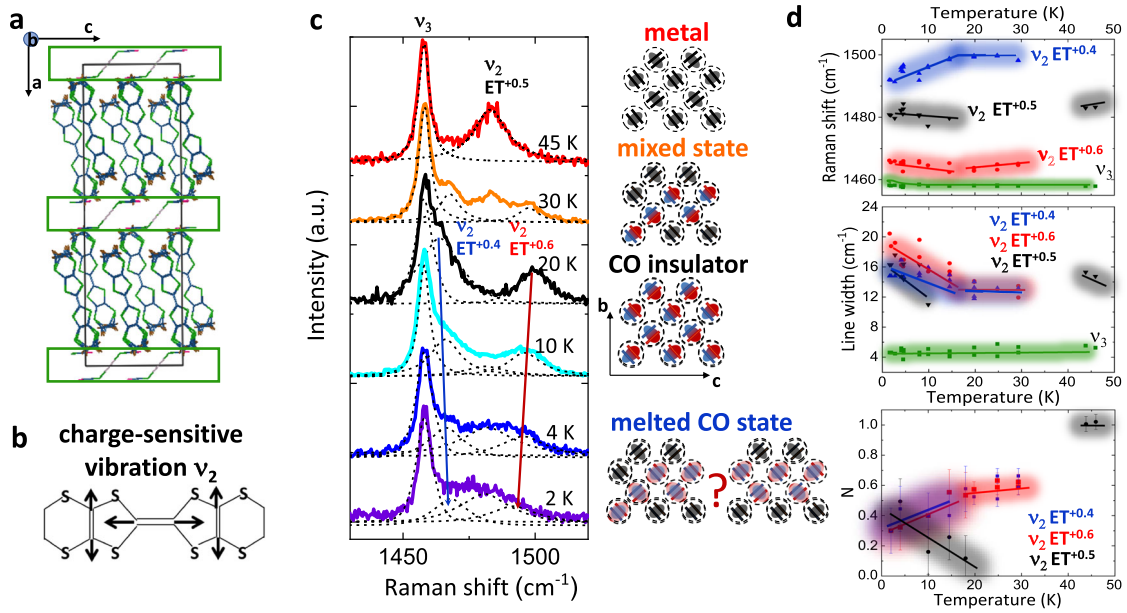

Fig. 1 Evidence of low temperature charge order melting in κ-(BEDT-TTF$_2$)Hg(SCN)$_2$Cl provided by vibrational Raman spectrocopy. **a** Layered crystal structure of quasi-two-dimensional (quasi-2D) molecular-based Mott insulators. **b** Eigenvectors of charge-sensitive molecular vibration ν_2. **c** Raman spectra of κ-Hg-Cl in the spectral range of the charge-sensitive vibration ν_2 at different temperatures. Drawings on the right represent the charge distribution on the lattice, black is for BEDT-TTF$^{+0.5}$, red for BEDT-TTF$^{+0.6}$, and blue is for BEDT-TTF$^{+0.4}$; ET = BEDT-TTF on the plots. From the top to the bottom: In the metallic state at 45 K only ν_2(BEDT-TTF$^{+0.5}$) is observed; at the temperature of charge order transition T_{CO}=30 K a mix of metallic domains with ν_2(BEDT-TTF$^{+0.5}$) and charge ordered domains with ν_2(BEDT-TTF$^{+0.6}$)/ν_2(BEDT-TTF$^{+0.4}$) is observed; in the charge ordered state at $T = 20$ K ν_2(BEDT-TTF$^{+0.6}$) and ν_2(BEDT-TTF$^{+0.4}$) are observed; at $T = 10$ K charge order starts to melt, broadened ν_2(BEDT-TTF$^{+0.6}$)/ν_2(BEDT-TTF$^{+0.4}$), and weak ν_2(BEDT-TTF$^{+0.5}$) are observed, a fraction of molecules corresponding to BEDT-TTF$^{+0.5}$ is about 0.2 of the whole system; at $T = 4$ and 2 K broadened ν_2(BEDT-TTF$^{+0.6}$)/ν_2(BEDT-TTF$^{+0.4}$), and ν_2(BEDT-TTF$^{+0.5}$) are observed, ~0.3 of the system has each charge state. **d** Temperature dependence of the frequencies (upper panel) and line width (middle panel) of ν_2 and ν_3. Note the splitting of ν_2 band below 30 K, and then broadening and change of frequencies which reduces the difference between $\nu_2(A)$ and $\nu_2(B)$. The lower panel shows a temperature dependence of the fraction of the system **N** associated with different charges on BEDT-TTF molecule. See Methods for the details of calculations and error bars definition.

scattering intensity $\chi''(\omega)$ flattens due to the suppression of spectral weight (Fig. 2a, ref. [18]). This estimate yields 2Δ of ~300 cm^{-1}. An opening of an insulating gap due to electronic correlations can be observed by Raman scattering in strongly correlated materials, for example in SmB_6[19,20]. Both experiment[19,21] and theory[20] agree that such a gap is observed in B_{1g} channel for D_{4h} point group, which corresponds to the (b,c) scattering channel for κ-Hg-Cl.

A broad asymmetric feature appears in the spectra below $T_{CO} =$ 30 K at about 420 cm^{-1} in (b,c), and (b,b) scattering channels, while its intensity in (c,c) is negligible (see Fig. 2b). The exact details of the origin of this feature are outside of the scope of this paper; its position suggests that it originates from a coupling of electrons to a vibration of BEDT-TTF molecule[22]. The negligible intensity of this feature in the (c,c) scattering channel which corresponds to the direction of the charge stripes demonstrates the anisotropy of the charge ordered system.

This experimental evidence for effective dimensionality reduction from 2D to 1D in κ-Hg-Cl due to the electric dipole order below $T_{CO} = 30$ K is in agreement with the previous reports[10,11], and with recent DFT calculations[23]. In the absence of a coupling to the lattice, the charge-rich stripes with unpaired spins can be considered as 1D antiferromagnetic (AF) chains[15]. $S = 1/2$ 1D spin chains with antiferromagnetic nearest neighbor coupling between spins have a potential to show spin liquid properties[24]. On the other hand, in a strong coupling to the lattice regime, charge-rich sites presumably will form spin singlet state[25]. Our study does not observe any major changes for lattice phonons on the charge order transition at 30 K (for details see SI). This confirms the results of XRD measurements[10], and suggests weak coupling of the charge order to the lattice.

Typically, a broken symmetry state would be a ground state of a system. However, for κ-Hg-Cl we observe melting of the charge order below ~15 K. The first evidence comes from vibrational spectroscopy: the components of the charge sensitive band ν_2 start to gradually broaden, move closer together in frequencies, and loose spectral weight to the increasing intensity of ν_2 (BEDT-TTF$^{+0.5}$). An appearance of ν_2 (BEDT-TTF$^{+0.5}$) suggests a recovery of homogeneous charge distribution for part of the system. This will correspond to a disappearance of electric dipoles on (BEDT-TTF)$_2$ sites. Based on the temperature dependence of the intensity of ν_2 band for different charges on BEDT-TTF molecule (see Methods for details), we can estimate a dependence of fractions N of differently charged BEDT-TTF molecules on temperature, as presented in Fig. 1d, lower panel.

At T = 10 K the estimated distribution is: $N(+0.4e) : N(+0.6e) : N(+0.5e) = 0.4 \pm 0.15 : 0.4 \pm 0.15 : 0.16 \pm 0.15$. The loss of charge order is accompanied by a decrease of the spectral weight of the 420 cm^{-1} mode: ~20% spectral weight reduction for this mode at 10 K ($I(10\,\mathrm{K}) = 0.82I(20\,\mathrm{K})$) is in agreement with a charge order loss in about 0.16 of molecular dimers as estimated by ν_2 mode analysis. While losing spectral weight, the feature at 420 cm^{-1} preserves the anisotropy related to the charge stripes along c-axis. The electronic gap does not change below the charge order transition at 30 K (Fig. 2a). No major changes in vibrational features apart from ν_2 are observed, confirming again that the coupling of the charge order to the lattice is weak.

At the lowest measured temperature of 2 K it is difficult to distinguish single components of ν_2 mode, which shows intensity spread from ~1450–1510 m^{-1}. If we identify the components of ν_2 in a way similar to the 10 K data analysis, we can estimate that the

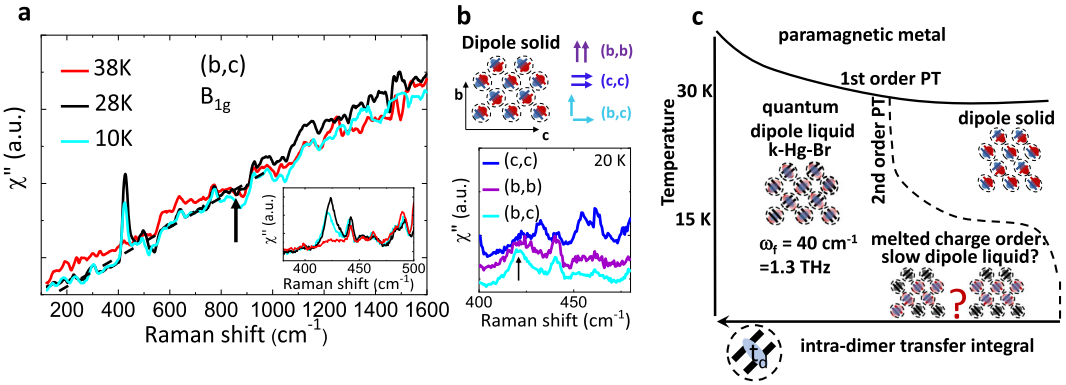

Fig. 2 Electronic gap in κ-(BEDT-TTF)$_2$Hg(SCN)$_2$Cl observed by Raman spectrocopy, and a schematic phase diagram suggested for this class of materials as a function of temperature and overlap integral in a dimer (BEDT-TTF)$_2$. a Electronic scattering of κ-Hg-Cl in B_{1g} scattering channel in metallic state ($T = 38$ K), charge ordered state ($T = 28$ K), and at $T = 10$ K with ~0.16 of the charge order melted. A gap opens on the transition into the charge ordered state and is preserved at $T = 10$ K. The arrow in the plot marks the isosbestic point in the spectra, while the gap itself is smaller and is estimated to be of about 300 cm^{-1}. The black dashed line is a guide for the eyes to identify the spectral region where frequency dependence of Raman intensity $\chi''(\omega)$ flattens due to the gapped density of states. The inset shows a new anisotropic mode which appears in the spectra of the charge ordered state, see text for details. Note the decrease of the intensity of this mode at changing the temperature from 28 to 10 K. **b** Upper panel: a scheme of orientation of light polarization with respect to the lattice of κ-Hg-Cl with charge stripes along *c* axis. Lower panel: polarization dependence of the feature at about 420 cm^{-1} at 20 K. This feature appears in the spectra in the charge ordered phase. Note the anisotropy of the mode. **c** Suggested schematic phase diagram where overlap integral in a dimer t_d controls a quantum phase transition between dipole (charge) order and non-charge-ordered Mott insulator phase. A phase transition on lowering temperature is of the first order (solid line), while a phase transition controlled by t_d is a second order transition (dashed line).

charge distribution is: $N(+0.4e) : N(+0.6e) : N(+0.5e) = 0.3 \pm 0.15 : 0.3 \pm 0.15 : 0.3 \pm 0.15$.

The shape of the ν_2 line in the low-temperature phase of κ-Hg-Cl was reproduced on different cooling cycles, and at cooling rates ranging between 0.1 K/min to 40 K/min in measurements with two different laser probes, a circular-shaped probe with a diameter of 2 μm, and elliptically shaped probe with diameters of 50 and 100 μm. Thus, if the mixture is formed by domains, they are much smaller than 2 μm.

The width of ν_2 line components increases gradually on cooling into the melted charge order regime. This is in contrast to the spectra of a mixed state that consists of metallic and charge ordered domains observed at the temperature of the charge order phase transition $T = 30$ K (see Fig. 1b). Those spectra show a superposition of charge-homogeneous and charge ordered responses without an additional broadening of vibrational lines. Such a formation of local strain-controlled domains on a phase transition into a charge ordered insulating phase was observed in α-(BEDT-TTF)$_2$I$_3$[26]. Typically, domains formed at a phase transition in BEDT-TTF-based materials vary in size from ~1 μm[26]–100 μm[27].

DISCUSSION

As our data show, an interplay between electronic correlations and frustration of the lattice leads to exotic effects related to the metal-insulator transition and insulating state. The charge order in κ-Hg-Cl is weakly coupled to the lattice, which explains an absence of a spin singlet state[28,29].

Our main result shows that the charge order observed at temperatures below $T = 30$ K is not the ground state of the system. On cooling below 15 K charge order gradually melts with part of the system recovering homogeneous distribution of charge on the lattice. A fraction of the system which still holds charge order shows broadened charge-sensitive ν_2 vibrational modes shifting closer together in frequency on cooling. This gradual melting of charge order does not have a detectable effect on heat capacity[6]. We find no dependence on cooling rate, or any other evidence for charge glass behavior. The melting of charge order occurs without a formation of macroscopic domains of different phases. The low-temperature state can be interpreted as a charge-fluctuating or microscopically disordered charge state.

Based on vibrational spectroscopy alone it is not possible to distinguish a decrease of charge disproportionation accompanied by some additional charge disorder from an offset of slow charge fluctuations. However, a continuous change of the line positions and width on cooling is in better agreement with melting of charge order through a development of charge fluctuations. A frequency of charge fluctuations or, in other words, dipole fluctuations in this case is about 4 cm^{-1} at 2 K, according to the line width analysis[6]. This is an order of magnitude slower than dipole fluctuations observed in the quantum dipole liquid κ-(BEDT-TTF)$_2$Hg(SCN)$_2$Br. A fraction of the system which preserves this charge order also preserves 1D anisotropy, as indicated by anisotropic Raman response at 420 cm^{-1}. We estimate that at the lowest measured temperature of 2 K each charge state presents ~1/3 of the system.

Our results demonstrate the low-temperature melting of the dipole order in κ-Hg-Cl, but some published experimental data for this material also reveal the low-temperature re-entrant-like behavior. Resistivity of κ-Hg-Cl[10,11,30,31] increases by a few orders of magnitude on the metal-insulator transition at 30 K, but the temperature dependence flattens below 20 K, which is apparently related to the charge order melting regime. Published ESR data[11,32] reveal a metal-insulator transition around 30 K, and another change of behavior at about 20 K. The overall temperature behavior is in agreement with our findings, while the details of interpretation can be revised based on the new information about the charge state in κ-Hg-Cl provided in this work.

There is a number of models which can be relevant to our observations on the melting of the charge order in the low-temperature phase of κ-Hg-Cl. None of them describe our results in full:

A re-entrant transition is predicted for a system with electronic ferroelecticity of molecular dimers in ref. [33]. It is suggested that on lowering the temperature, antiferromagnetic exchange would compete with the interactions which lead to ferroelectric order, and weaken them, leading to the loss of the ferroelectric order and 120° spin order. The latter has not been observed experimentally for κ-Hg-Cl[28,29].

A number of models for a frustrated charge system discuss a competition between stripes charge order similar to that found in κ-Hg-Cl below $T_{MI} = 30$ K, and different variants of a three-fold

charge order. This phase competition at low temperatures can result in a melting of a ferroelectric charge order state without an impact of magnetic interactions. Yoshida and Hotta[34] discuss a competition between charge order stripes and an "order by disorder" phase with so-called "good defects" containing ordered pairs produced by thermal fluctuations. Another possibility is a competition between ferroelectric stripes and anti-ferroelectric three-fold stripes ground state discussed in refs [15,35]. Interestingly, a competition between ferroelectric and antiferroelectic state is a reason for quantum paraelectric behavior in $SrTiO_3$[36].

Our experimental data present a limited agreement with these models, without suggesting a clear picture. It is worth noting here, that no magnetic order has been found so far in these systems down to ~100 mK[29]. At 2 K we observe a charge distribution which corresponds to a three-fold charge order, but it is not clear if this charge distribution is the final state of the system or it would change on cooling. In the melted state, the 1D anisotropy is preserved for a fraction of the system which holds charge separation. This is in agreement both with a scenario that involves a competition of different stripe orders, and with a presence of microscopic domains containing stripes on a re-entrant transition. Three-fold charge order is predicted to be a metallic state, and the stripe order of this kind is antiferroelectric and thus would change the dielectric constant behavior. Further experimental studies such as detailed dielectric measurements and resistivity below 30 K are necessary for the identification of the low-temperature state.

The models discussed above work on the assumption that the ferroelectric state is static. Since the dielectric measurements are done at about 1000 kHz, and Raman and optical measurements are done at even higher frequencies, it cannot be excluded that very slow fluctuations, with frequencies below 100 kHz are present even between 30 and 20 K. This would suggest that the MI transition and the gap at about 300 cm^{-1} are related to purely Mott transition.

We find it useful to summarize our results on properties associated with a charge degree of freedom in κ-Hg-Cl and related materials in a schematic phase diagram drafted in Fig. 2c. It is known from previous work that a transition into insulating state on temperature lowering is of the first order for both κ-Hg-Cl[11], and the closely related quantum dipole liquid κ-$(BEDT\text{-}TTF)_2Hg(SCN)_2Br$[6,37]. The fluctuations of the charge order in κ-$(BEDT\text{-}TTF)_2Hg(SCN)_2Br$, and dipole ordered phase or possibly much slower fluctuations in κ-Hg-Cl suggest a quantum critical point and a second order phase transition into a charge ordered state. According to theoretical models[5,33,38], and DFT calculations of electronic parameters[11](Valenti, R. Private communication), the tuning parameter of the ground state is the overlap integral t_d in a $(BEDT\text{-}TTF)_2$ dimer[5,6]. A similar phase diagram with 1st order phase transition on lowering temperature, and 2nd order phase transition on a variation of another parameter, as well as a relevant triple quantum critical point is suggested for ferroelectrics such as $SrTiO_3$ without spin degree of freedom[36].

METHODS

Synthesis

Single crystals of κ-$(BEDT\text{-}TTF)_2Hg(SCN)_2Cl$ (κ-Hg-Cl) were prepared by electrochemical oxidation of the BEDT-TTF solution in 1,1,2-trichloroethane (TCE) at a temperature of 40° C and a constant current of 0.5 μA. A solution of $Hg(SCN)_2$, $[Me_4N]SCNKCl$, and dibenzo-18-crown-6 in 1:0.7:1 molar ratio in ethanol/TCE was used as supporting electrolyte for the κ-Hg-Cl preparation. The composition of the crystals was verified by electron probe microanalysis and X-ray diffraction.

Raman scattering spectra were measured in three different setups.

(1) Spectra in the frequency range from 100 to 2000 cm^{-1} and at temperatures down to 10 K were measured in the pseudo-Brewster angle geometry using T64000 triple monochromator spectrometer equipped with the liquid N_2 cooled CCD detector. In single monochromator configuration an edge filter option was used. Spectral resolution was 2 cm^{-1}. Line of Ar^+-Kr^+ Coherent laser at 514 nm was used for excitation. Laser power was kept at 2 mW for an elliptical laser probe with diameters of 50 μm and 100 μm. This ensured that laser heating of the sample was kept below 2 K, as was proved by observing the temperature of ordering transition in κ-Hg-Cl at 30 K, in agreement with heat capacity measurements. Measurements at temperatures down to 10 K were performed using Janis ST500 cold finger cryostat. Cooling rates used were between 0.1 and 40 K/min. The samples were glued on the cold finger of the cryostat using GE varnish.
(2) Non-polarized micro-Raman measurements in the range of charge-sensitive vibrations were performed in backscattering geometry using T64000 triple monochromator spectrometer equipped with the Olympus microscope. Probe size was 2 μm in diameter.
(3) Measurements down to 1.9 K in the spectral range between 1200 and 1700 cm^{-1} with a spectral resolution of 1.74 cm^{-1} were conducted at National High Magnetic Field Lab (NHMFL). The Raman spectra were measured in a backscattering geometry using a 532-nm laser excitation. The laser light was injected into a single mode optical fiber, guiding the excitation to the sample stage inserted into a helium-flow variable temperature cryostat with exchange gas sample environment. The excitation light was focused by an aspheric objective lens (NA = 0.67) to a spot size of ~3.5 μm in diameter. The excitation power delivered to the sample was ~100 μW or less to minimize the sample heating. The scattered light collected by the same lens was directed into a 100-μm multimode collection fiber, and then guided to a spectrometer equipped with a liquid-nitrogen-cooled CCD camera.

These different measurements were performed on at least 6 samples to ensure reproducibility of the results. We demonstrate original data from four different measurements done on three different samples in the Supplemental Information, Fig. 2.

The crystals were oriented using polarization-dependent Raman scattering measurements. For the measurements, electrical vectors of excitation e_L and scattered e_S light were polarized along b and c axes. Our notations of polarizations refer to the structure and symmetry of the BEDT-TTF layer, to make an easy comparison to the calculations for D_{4h} point group symmetry[20]. Thus, A_{1g} symmetry corresponds to the measurements done in (b, b) and (c, c) geometries, and B_{1g} corresponds to measurements done in (b, c) and (c, b) geometries, see[39] for more detailed information. All spectra were corrected by the Bose-Einstein thermal factor.

Data analysis

We determine charge on BEDT-TTF molecules in κ-Hg-Cl crystals by following the frequency of the central C = C molecular bond vibration (ν_2) (Fig. 1b, c). This frequency changes by ~−140 cm^{-1} when charge on a molecule changes from $(BEDT\text{-}TTF)^0$ to $(BEDT\text{-}TTF)^{+1}$, as demonstrated in refs [40,41]. This is a result of a lengthening of the central C=C bond of the molecule when more charge occupy the highest occupied molecular orbital (HOMO).

To compute fractions of the system N, that carry different charges at temperatures below 30 K (see Fig. 1d lower panel), we performed a comparative analyses of Raman intensities. While the frequency of the ν_2 charge sensitive vibration depends linearly on the charge of a BEDT-TTF molecule[41], the Raman intensity shows a non-linear dependence, which we obtained from the experiment. The known points of this dependence is at $T = 45$ K in the metallic state, where all molecules have on average $+0.5e$ charge, and *at* $T = 22$ K, where half of the system carriers charge $+0.6e$, and the other half carries $+0.4e$. Spectral weight of ν_2 vs Raman shift plot is presented in Fig. 3. In the plot, spectral weight was calculated by fitting the vibrational bands by a Lorentzian function, and normalized to the spectral weight of ν_3 C=C non-charge sensitive band, in order to correct for the errors of intensity measurements at different temperatures. Intensity deviations can occur due to small misalignments of a measurement system on changing the temperature. We used the empirical dependency (solid line) to estimate the fraction N of BEDT-TTF molecules carrying a certain charge at temperatures below 15 K. Error bars in Fig. 1d lower panel were determined though an estimation of the respective error in calculation of the spectral weight of a vibrational line.

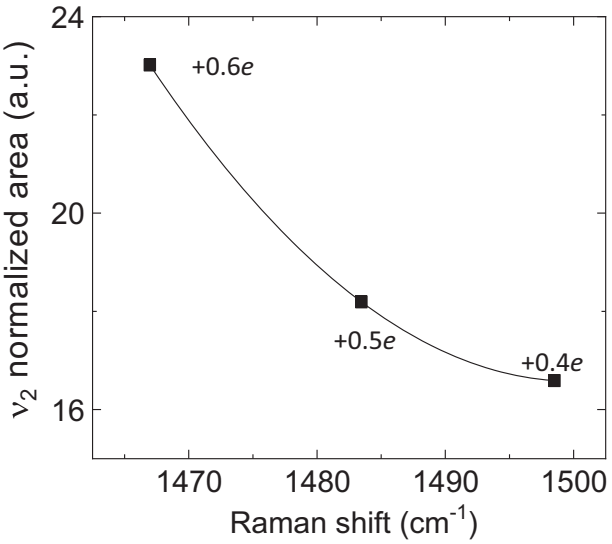

Fig. 3 Dependence of normalized intensity of a charge sensitive mode ν_2 of BEDT-TTF molecule on Raman shift. The latter is defined by the charge on the molecule. Points represent the known values of BEDT-TTF average charge.

DATA AVAILABILITY

The data that support the findings of this study are available from the corresponding author upon reasonable request.

Received: 17 June 2019; Accepted: 29 January 2020;
Published online: 06 March 2020

REFERENCES

1. Sato, T., Miyagawa, K. & Kanoda, K. Electronic crystal growth. *Science* **357**, 1378–1381 (2017).
2. Sasaki, S. et al. Crystallization and vitrification of electrons in a glass-forming charge liquid. *Science* **357**, 1381–1385 (2017).
3. Yao, N. Y., Zaletel, M. P., Stamper-Kurn, D. M. & Vishwanath, A. A quantum dipolar spin liquid. *Nat. Phys.* **14**, 405–410 (2018).
4. Shen, S.-P. et al. Quantum electric-dipole liquid on a triangular lattice. *Nat. Commun.* **7**, 10569 (2016).
5. Hotta, C. Quantum electric dipoles in spin-liquid dimer Mott insulator κ-ETκCuκ (CN)κ. *Phys. Rev. B* **82**, 241104 (2010).
6. Hassan, N. et al. Evidence for a quantum dipole liquid state in an organic quasi-two-dimensional material. *Science* **360**, 1101–1104 (2018).
7. Dunnett, K., Zhu, J.-X., Spaldin, N., Juričić, V. & Balatsky, A. V. Dynamic multiferroicity of a ferroelectric quantum critical point. *Phys. Rev. Lett.* **122**, 057208 (2019).
8. Naka, M. & Ishihara, S. Quantum melting of magnetic order in an organic dimer mott-insulating system. *Phys. Rev. B* **93**, 195114 (2016).
9. Naka, M. & Ishihara, S. Magnetoelectric effect in organic molecular solids. *Sci. Rep.* **6**, 20781 (2016).
10. Drichko, N. et al. Metallic state and charge-order metal-insulator transition in the quasi-two-dimensional conductor κ-(BEDT-TTF)^{2}Hg(SCN)^2 Cl. *Phys. Rev.B* **89**, 075133 (2014).
11. Gati, E. et al. Evidence for electronically driven ferroelectricity in a strongly correlated dimerized BEDT-TTF molecular conductor. *Phys. Rev. Lett.* **120**, 247601 (2018).
12. Merino, J., Greco, A., McKenzie, R. H. & Calandra, M. Dynamical properties of a strongly correlated model for quarter-filled layered organic molecular crystals. *Phys. Rev. B* **68**, 245121 (2003).
13. Murray, J. M. & Tešanović, Z. Theory of charge order and heavy-electron formation in the mixed-valence compound KNi_2Se_2. *Phys. Rev. B* **87**, 081103 (2013).
14. Neilson, J. R. et al. Local increase of symmetry on cooling in KNi_2Se_2. https://arxiv.org/abs/1310.6828 (2013).
15. Watanabe, H. & Seo, H. Phase competition and superconductivity in κ-(BEDT-TTF)^{2}X: Importance of intermolecular coulomb interactions. *J. Phys. Soc. Jpn* **86**, 033703 (2017).
16. Drichko, N. et al. Electronic properties of correlated metals in the vicinity of a charge-order transition: optical spectroscopy of α-(BEDT-TTF)^{2}MHg(SCN)^4(M= Nh^4, Rb, Tl). *Phys. Rev.* **74**, 235121 (2006).
17. Yakushi, K., Yamamoto, K., Yamamoto, T., Saito, Y. & Kawamoto, A. Raman spectroscopy study of charge fluctuation in the spin-liquid candidate κ-BEDTTTF) κCuκ(CN)κ. *J. Phys. Soc. Jpn* **84**, 084711 (2015).
18. Nyhus, P., Cooper, S. L., Fisk, Z. & Sarrao, J. Low-energy excitations of the correlation-gap insulator SmB_6: a light-scattering study. *Phys. Rev. B* **55**, 12488 (1997).
19. Valentine, M. E. et al. Breakdown of the Kondo insulating state in SmB_6: a light-scattering study. *Phys. Rev. B* **94**, 075102 (2016).
20. Devereaux, T. P. & Hackl, R. Inelastic light scattering from correlated electrons. *Rev. Mod. Phys.* **79**, 175 (2007).
21. Caprara, S. et al. Signatures of nematic quantum critical fluctuations in the raman spectra of lightly doped cuprates. *Phys. Rev. B* **91**, 205115 (2015).
22. Eldridge, J., Homes, C., Williams, J. M., Kini, A. & Wang, H. H. The assignment of the normal modes of the BEDT-TTF electron-donor molecule using the infrared and raman spectra of several isotopic analogs. *Spectrochim. Acta A Mol. Biomol. Spectrosc.* **51**, 947–960 (1995).
23. Jacko, A., Kenny, E. & Powell, B. Interplay of dipoles and spins in κ-(BEDT-TTF)$_2$*X*, where X = Hg(SCN)$_2$Cl, Hg(SCN)$_2$Br, Cu[N(CN)$_2$]Cl, Cu[N(CN)$_2$]Br, and Ag$_2$(CN)$_3$. https://arxiv.org/abs/1909.10755 (2019).
24. Mila, F. Quantum spin liquids. *Eur. J. Phys.* **21**, 499–510 (2000).
25. Dayal, S., Clay, R. T., Li, H. & Mazumdar, S. Paired electron crystal: Order from frustration in the quarter-filled band. *Phys. Rev. B* **83**, 245106 (2011).
26. Pustogow, A., McLeod, A., Saito, Y., Basov, D. & Dressel, M. Internal strain tunes electronic correlations on the nanoscale. *Sci. Adv.* **4**, eaau9123 (2018).
27. Sasaki, T., Yoneyama, N., Kobayashi, N., Ikemoto, Y. & Kimura, H. Imaging phase separation near the mott boundary of the correlated organic superconductors κ-(BEDT-TTF)κX. *Phys. Rev. Lett.* **92**, 227001 (2004).
28. Yamashita, M. & Drichko, N. In preparation (2019).
29. Pustogow, A. et al. Impurity moments conceal low-energy relaxation of quantum spin liquids. Preprint at https://arxiv.org/abs/1911.02057 (2019).
30. Thomas, T. et al. Low-frequency charge carrier dynamics in ferroelectric κ-(BEDT-TTF)^{2}X-a comparative study of X = Cu[N(CN)^2]Cl and X = Hg(SCN)^{2}Cl. *Phys. Stat. Solidi (b)* **256**, 1800746 (2019).
31. Ivek, T. et al. Metal-insulator transition in the dimerized organic conductor κ-(BEDT-TTF)κ-Hg(SCN)κ-Br.*Phys. Rev. B* **96**, 085116 (2017).
32. Yasin, S. et al. Electronic and magnetic studies of κ-(BEDT-TTF)^{2}Hg(SCN)κCl. *Phys. B Condens. Matter* **407**, 1689–1691 (2012).
33. Naka, M. & Ishihara, S. Electronic ferroelectricity in a dimer Mott insulator. *J. Phys. Soc. Jpn* **79**, 063707 (2010).
34. Yoshida, T. & Hotta, C. Frustrated electrons on a spatially anisotropic triangular lattice: emergent competition of charge orders and exotic disorders due to thermal fluctuations. *Phys. Rev. B* **90**, 245115 (2014).
35. Mori, T. Non-stripe charge order in dimerized organic conductors. *Phys. Rev. B* **93**, 245104 (2016).
36. Chandra, P., Lonzarich, G. G., Rowley, S. & Scott, J. Prospects and applications near ferroelectric quantum phase transitions: a key issues review. *Rep. Progr. Phys.* **80**, 112502 (2017).
37. Hemmida, M. et al. Weak ferromagnetism and glassy state in κ-(BEDT-TTF)^2-Hg(SCN)^2-Br. *Phys. Rev. B* **98**, 241202 (2018).
38. Sato, N., Watanabe, T., Naka, M. & Ishihara, S. Spin and charge fluctuations near metal-insulator transition in dimer-type molecular solid. *J. Phys. Soc. Jpn* **86**, 053701 (2017).
39. Drichko, N., Hackl, R. & Schlueter, J. A. Antiferromagnetic fluctuations in a quasi-two-dimensional organic superconductor detected by raman spectroscopy. *Phys. Rev. B* **92**, 161112 (2015).
40. Dressel, M & Drichko, N. Optical properties of two-dimensional organic conductors: signatures of charge ordering and correlation effects. *Chem. Rev.* **104**, 5689–5716 (2004).
41. Yamamoto, T. et al. Examination of the charge-sensitive vibrational modes in bis (ethylenedithio) tetrathiafulvalene. *J. Phys. Chem. B* **109**, 15226–15235 (2005).

ACKNOWLEDGEMENTS

We are grateful to T. Clay, T. Mori, C. Hotta, H. Seo, M. Naka, T. Ivek, and M. Yamashita for fruitful discussions. Work at JHU was supported as part of the Institute for Quantum Matter, an Energy Frontier Research Center funded by the U.S. Department of Energy, Office of Science, Office of Basic Energy Sciences under Award Number DE-SC0019331. The work in Chernogolovka was supported by FASO Russia, state registration number 0089-2019-0011. K.T. acknowledges funding via ONR HBCU/MI program. A portion of this work was performed at the National High Magnetic Field Laboratory, which is supported by the National Science Foundation Cooperative Agreement No. DMR-1644779 and the State of Florida. N.D. and N.M.H. acknowledge

the support of Institute for Complex Adaptive Matter (ICAM) and The Gordon and Betty Moore Foundation.

AUTHOR CONTRIBUTIONS

N.M.H. performed Raman scattering experiments and data analysis, K.T. and Zh.L. performed Raman scattering experiments in NHMFL, D.S. assisted performing Raman scattering experiments in NHMFL, E.I.Z, S.T., and R.N.L synthesized samples, N.D. conceived the experiments, performed Raman scattering measurements and data analysis, wrote the paper.

COMPETING INTERESTS

The authors declare no competing interests.

ADDITIONAL INFORMATION

Supplementary information is available for this paper at https://doi.org/10.1038/s41535-020-0217-5.

Correspondence and requests for materials should be addressed to N.D.

Reprints and permission information is available at http://www.nature.com/reprints

Publisher's note Springer Nature remains neutral with regard to jurisdictional claims in published maps and institutional affiliations.